CODAR: A Contextual Duration-Aware Qubit Mapping for Various NISQ Devices

Haowei Deng, Yu Zhang* and Quanxi Li

School of Computer Science and Technology, University of Science and Technology of China, Hefei, China

Email: jackdhw@mail.ustc.edu.cn, yuzhang@ustc.edu.cn*, crazylqx@mail.ustc.edu.cn

Abstract—Quantum computing devices in the NISQ era share common features and challenges like limited connectivity between qubits. Since two-qubit gates are allowed on limited qubit pairs, quantum compilers must transform original quantum programs to fit the hardware constraints. Previous works on qubit mapping assume different gates have the same execution duration, which limits them to explore the parallelism from the program. To address this drawback, we propose a Multi-architecture Adaptive Quantum Abstract Machine (maQAM) and a COntext-sensitive and Duration-Aware Remapping algorithm (CODAR). The CODAR remapper is aware of gate duration difference and program context, enabling it to extract more parallelism from programs and speed up the quantum programs by 1.23 in simulation on average in different architectures and maintain the fidelity of circuits when running on OriginQ quantum noisy simulator.

I. INTRODUCTION

Quantum Computing (QC) has attracted huge attention in recent a decade due to its ability to exponentially accelerate some important algorithms [22]. Both QC algorithm designers and programmers work at a very high level, and know little about (future) NISQ devices that (will) execute quantum programs. There exists a gap, however, between NISQ devices and the hardware requirements (*e.g.,* size and reliability) of QC algorithms. To bridge the gap, QC requires abstraction layer and toolchain to translate and optimize quantum programs [8]. QC compilers typically translate high-level QC code into (optimized) circuit-level assembly code in multiple stages.

In order to use NISQ hardware, quantum circuit programs have to be compiled to the target device, which includes mapping logical qubits to physical ones of the device. The mapping step, which we focus on in this paper, faces a tough challenge because further physical constraints have to be considered. In fact, 2-qubit gates can only be applied to certain physical qubit pairs. A common method to solve this problem is to insert additional SWAP operations in order to "move" the logical qubits to positions where they can interact with each other. This qubit mapping problem has been proved to be a NP-Complete problem [26].

Previous solutions to this problem can be classified into two types. One of them is to formulate the problem into an equivalent mathematical problem and apply a solver [6, 7, 23, 29, 30, 32] and the other type is to use heuristic search to obtain approximate results [5, 15, 16, 18, 33, 35]. The former suffers from a very long runtime and can only apply to small-size cases. The latter is better in runtime, especially when the circuit is large scale. All these algorithms assume that different gates have the same execution duration.

On NISQ hardware, however, different gates have different durations (see Table I). Ignoring the gate duration difference may cause these algorithms to find the shortest depth but not the shortest execution time. The real execution time of the circuit is associated with the weighted depth, in which different gates have different duration weights. Considering gate duration difference will help the compiler make better use of the parallelism of quantum circuits and generate circuits with shorter execution time.

In this paper, we focus on solving the *qubit mapping problem* by heuristic search with the consideration of gate duration difference and program context to explore more program's parallelism. To address the challenges of qubit mapping problem and adapt to different quantum technologies, we first give several examples to explain our motivation, then propose a **M**ulti-architecture **A**daptive **Q**uantum **A**bstract **M**achine (maQAM) for studying the qubit mapping problem. The maQAM is modeled as a coupling graph with limited qubit connectivity and configurable durations of different kinds of quantum gates. Based on the maQAM, we further propose two mechanisms that enable **CO**ntext-sensitive and **D**uration-**A**ware **R**emapping algorithm (CODAR) to solve the qubit mapping problem with the awareness of gate duration difference and program context.

The main contributions of this paper are as follows:

- We summarize the features of different QC technologies including their available gates, operation fidelity and execution duration, and establish the quantum architecture abstraction with configurable parameters – maQAM.
- We propose a SWAP-based heuristic algorithm for qubit remapping, CODAR, which considers the gate duration difference and program context and can further speed up the quantum program.
- We evaluate CODAR with various benchmarks on several latest hardware models such as Google's 54-qubit Sycamore processor [3]. Experimental results show that CODAR speeds up quantum programs by 1.212∼1.258 at the average in comparison with the best-known algorithm, and maintains the fidelity of circuits when running on OriginQ quantum noisy simulator [24].

II. PROBLEM ANALYSIS

A. Recent Work on Qubit Mapping

There are a lot of research on the qubit mapping problem. Here we focus on analyzing some valuable solutions in recent two years [4, 18, 21, 26, 28, 32, 35]. All of them are proposed for some IBM QX architectures, and none of them consider the gate duration difference.

a) Solutions only considering qubit coupling: [26, 32] provide solutions for 5-qubit IBM QX architectures with directed coupling. Siraichi *et al.* [26] propose an optimal algorithm based on dynamic programming, which only fits for small circuits; then they propose a heuristic one which is fast but oversimplified with results worse than IBM's solution. Wille *et al.* [32] present a solution with a minimal number of additional SWAP and H operations, in which qubit mapping problem is formulated as a symbolic optimization problem with high complexity. They utilize powerful reasoning engines to solve the computationally task.

[18, 35] use heuristic search to provide good solutions in acceptable time for large scale circuits. Zulehner *et al.* [35] divide the two-qubit gates into independent layers, then use A^* search plus heuristic cost function to determine compliant mappings for each layer. Li *et al.* [18] propose a SWAP-based bidirectional heuristic search algorithm – SABRE, which can produce comparable results with exponential speedup against previous solutions such as [35].

TABLE I: Parameter information of several quantum computing devices.

		Ion Trap		Superconducting			Neutral Atom [25]
		Ion Q5 [19]	Ion Q11 [34]	IBM Q5 [19]	IBM Q16 [21]	IBM Q20 [18]	
Available 1-qubit gate		R^{θ}_{α}		X, Y, Z, H, S, T			R^{θ}_{α}
Available 2-qubit gate		XX		CNOT (CX)			CNOT (CX)[27]
Fidelity	1-qubit gate	99.1(5)%	99.5%	99.7%	∼99.8%	∼99.56%	99.995% [25]
	2-qubit gate	97(1)%	97.5%[95.1%,98.9%]	96.5%	∼96%	∼97%	82%[20]
	1-qubit readout	$\lvert 0\rangle$:99.7(1)%, $\lvert 1\rangle$:99.1(1)%	99.3%	∼ 96%	∼93%	∼91.2%	98.6% [12]
	average readout	95.7(1)%	–	∼ 80%	–	–	≥97.4(3)% [17]
Time	1-qubit gate	20μ s		130 ns	80 ns	–	1μ ∼20μ s
	2-qubit gate	250μ s	–	250-450 ns	170-391 ns	–	∼10μ s
Depolarization (T_1)		∼ ∞	–	∼ 60μ s	∼ 70μ s	87.29μ s	>10s
Spin dephasing (T_2)		∼ 0.5s	–	∼ 60μ s	∼ 70μ s	54.43μ s	∼ 1s

b) Solutions further considering error rates: [4, 21, 28] provide another type of perspective for solving the qubit mapping problem. They consider the variation in the error rates of different qubits and connections to generate directly executable circuits that improve reliability rather than minimize circuit depth and number of gates. Based on the error rate data from real IBM Q16 and Q20 respectively, [21, 28] use a SMT solver to schedule gate operations to qubits with lower error probabilities. Ash-Saki *et al.* propose two approaches, Sub-graph Search and Greedy approach, to optimize gate-errors [4]. Circuits generated by them may suffer from long execution time due to no consideration of the minimal circuit depth.

c) What we consider in the qubit mapping: We want to produce solutions for the qubit mapping problem with speedup against previous works and maintain the fidelity meanwhile. Besides the coupling map, what we further concern includes the program context and the gate duration difference, which affect the design of qubit mapping. Considering these factors will help to find remapping solution with approximate optimal execution close to reality.

B. Motivating Examples

We use several examples written in OpenQASM [10] to explain our motivation for considering program context and gate duration difference in the qubit remapping process. The two examples base on the coupling map of four physical qubits $Q_0 \sim Q_3$ and the assumed gate durations defined in Fig. 1 (a) and (b). We directly map the logical qubits q[0]∼q[3] initially to physical qubits $Q_0 \sim Q_3$ for easier explanation.
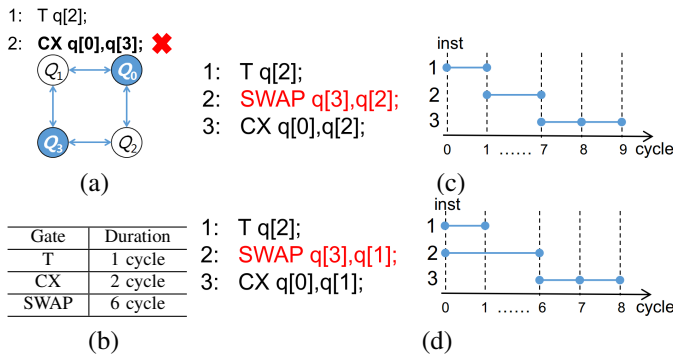

Fig. 1: An example reflecting the impact of **program context** on SWAP-based transformations: SWAP q[3], q[1] is selected in (d) to avoid using q[2] operated by the previous T gate, accordingly increasing parallelism.

a) Impact of program context: Consider the OpenQASM code fragment shown in Fig.1 (b). Since qubits Q_0 and Q_3 are non-adjacent, the instruction "CX q[0],q[3]" at line 2 cannot be applied. To solve the problem, SWAP operation is required before
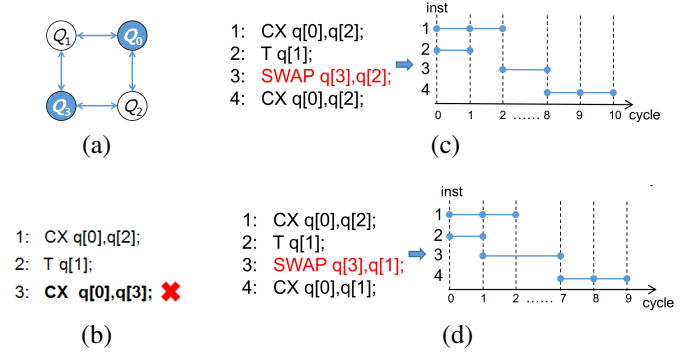

Fig. 2: A 4-qubit QFT example reflecting the impact of **gate duration difference**: "SWAP q[3],q[1]" is the best candidate since it can start immediately after "T q[1]" while "CX q[0],q[2]" has not finished yet, increasing the parallelism of the circuit.

performing the CX operation. In this case, there are four candidate SWAP pairs, *i.e.*, (Q_0, Q_1), (Q_0, Q_2), (Q_3, Q_1) and (Q_3, Q_2). If the program context, *i.e.*, the predecessor instruction "T q[2];", is not considered, there are no differences among the four candidates when selecting. However, SWAP operation on pair (Q_3, Q_2) or (Q_0, Q_2) conflicts with the context instruction "T q[2];" due to operating the same Q_2, and has to be executed serially after T operation as shown in Fig.1 (c). SWAP on pair (Q_3, Q_1) or (Q_3, Q_1) does not conflict with "T q[2];" and can be executed in parallel as shown in Fig.1 (d). With the awareness of the context information, SWAP operations that improve parallelism can be sifted out.

b) Impact of gate duration difference: We use a 4-qubit QFT (Quantum Fourier Transform) circuit to explain the limitation of ignoring the duration of quantum gates. Fig. 2 (b) lists the fragment of a 4-qubit QFT OpenQASM program, which is generated by ScaffCC compiler [2]. Similar to the first example, SWAP operation is required before performing the CX operation, and there are also the same four candidate SWAP pairs. Instructions "T q[2]" and "CX q[0],q[2]" can be executed in parallel and we assume both of them start at cycle 0. If the difference of gate durations is ignored, the two gates "T q[2]" and "CX q[0],q[2]" are assumed to finish at the same time t and the four candidate SWAP operations have to start after t. However, if the duration of CX is twice as much as that of T, we find that "T q[2]" will finish at cycle 1 while "CX q[0],q[2]" at cycle 2. As a result, SWAP between q[3] and q[1] can start at cycle 1 as shown in Fig.2 (d), while other three candidate SWAP operations have to start at cycle 2 since one of operands Q_0 or Q_2 is occupied as shown in Fig.2 (c). Fig. 2 (d) has better parallelism, which can be deduced by the awareness of different quantum gate durations.

TABLE II: Definition of Quantum Abstract Machine.

	Notation	Definition
Static Structure	Q_H	The set of physical qubits, $\|Q_H\| = N$; $\forall Q \in Q_H$, $Q.t_{end}$ is the qubit lock described in Section IV-A
	G	The set of elementary quantum operations and SWAP, $\|G\| = M$
	$\mathbb{M} = (Q_H, E_H)$	The coupling graph of a quantum device, $E_H \subseteq Q_H \times Q_H$
	$\tau: G \to \mathbb{N}$	Mapping from quantum operations to their durations, $\mathbb{N}$ represents the set of natural numbers
	$\mathbb{D}: Q_H \times Q_H \to \mathbb{N}$	Mapping from physical qubit pairs to their shortest path lengths on the $\mathbb{M}$, if there is no path between Q_i and Q_j, then $\mathbb{D}(Q_i,Q_j) = $ INT_MAX
Dynamic Structure	$\pi: Q_P \to Q_H$	Mapping from logical qubits to physical qubits
	CF(I)	Commutative Front gate set of a gate sequence I, defined in Definition 1
Auxiliary Functions	gate(g)	the name of a given gate g.
	qseq(g)	the logical qubit sequence applied by a given gate g.
Variables	$Q_{\{1,2,...,N\}}$	Physical qubits, $Q_i \in Q_H$, $1 \le i \le N$
	$q_{\{1,2,...,n\}}$	Logical qubits, $q_i \in Q_P$, $1 \le i \le n$
	$g_{\{1,2,...,M\}}$	Physical quantum operations, $g_i \in G$, $1 \le i \le M$
	$g_{\{1,2,...,m\}}$	Quantum operations in the circuit program
	I	A sequence of quantum operations, $I = [g_1, g_2, ..., g_k]$ if $k = \|I\|$, and the length of I is written as $I.len$

III. QUANTUM ARCHITECTURE ABSTRACTION

Since the qubit mapping problem is affected by the constraints of underlying QC devices, which based on various and evolving quantum technologies, it is essential to design quantum mapping algorithms that are compatible with different quantum technologies.

A. Characteristics of NISQ devices

Table I lists parameter information of some QC devices based on ion trap, superconducting and neutral atomic quantum technologies, respectively. From the table, we see that two-qubit gate executes slower (at least 2×) and has lower fidelity than single-qubit gate on both superconducting and ion trap platforms; the ion trap system is about 1000× slower than the superconducting system, but can execute more gates before decoherence. The directly implementable elementary gates in ion trap system are single-qubit gate R_α^θ (rotations by an angle θ about any axis α) and two-qubit gate XX. Specifically, CNOT gate can be implemented by a one-XX and four-R [11]. Neutral atoms are similar in magnitude to trapped ions. However, the two-qubit gate applied to neutral atoms may not perform slower than a single-qubit gate, but the fidelity is much worse.

B. Definition of the maQAM

In view of the above, we consider the qubit connectivity of various NISQ devices, and take each gate duration as a multiple of quantum clock cycle τ_u, which can be analogized to the classic clock cycle. We then introduce a **M**ulti-architecture **A**daptive **Q**uantum **A**bstract **M**achine (maQAM) which consists of static and dynamic structures, denoted as $\mathbb{A} = (A_s, A_d)$. Table II shows the definitions for maQAM, where $A_s = (Q_H, G, \mathbb{M}, \tau, \mathbb{D})$, and $A_d = (\pi, CF)$. We assume the device can provide enough physical qubits (denote the number as N) for the program's execution (denote the number of logical qubits in the program as n), *i.e., $N \ge n$.*

For a QC device, we abstract its qubit layout as a graph $\mathbb{M}$ where qubits are vertices and there are edges between qubit pairs where a two-qubit gate is allowed to apply on them. We introduce the Gate Duration Map τ into A_s which maps each kind of quantum gate to its duration, depending on the information from quantum architecture. We assume the same kind of quantum gates have the same duration and fidelity. We also introduce the shortest distance matrix map $\mathbb{D}$ between each pair of physical qubits for quick selection of exchangeable qubits in our CODAR scheduling algorithm.

IV. DESIGN OF THE QUBIT REMAPPING ALGORITHM

In this section, we discuss our design for **CO**ntext-sensitive and **D**uration-**A**ware **R**emapping algorithm (CODAR). We introduce two fundamental mechanisms that enable CODAR context-sensitivity and duration awareness, *i.e., qubit lock* and *commutativity detection*.

A. Qubit Lock

CODAR is based on a reasonable assumption: *Two or more gates cannot be applied to the same qubit at the same time*. If a gate occupies a qubit, we call the qubit busy, and other gates can no longer be applied to the qubit. As the example shown in Fig. 1, when inserting SWAP for a specific two-qubit gate CX q[0],q[3], the neighbour qubit q[2] of the target qubits may be occupied by the contextual gate which has started in an earlier time. Using the occupied qubits to route the two-qubit gate will reduce the parallelism of the program because the routing process has to wait until the occupied qubits become free.

To make CODAR aware of the qubit occupation by the past contextual gate, we introduce a **qubit lock** t_{end} for each physical qubit in Q. When start applying a quantum gate $g \in G$ whose duration is τ_g at time t to a physical qubit in Q, CODAR will update this qubit's t_{end} as $t + \tau_g$, which means the qubit is occupied before $t + \tau_g$. A qubit is *free* only when its lock $t_{end} \le$ current time, which means all the past gates applied on this qubit are finished. When trying to find a routing path for a specific two-qubit gate, by comparing t_{end} of each qubit with the current time, CODAR can be aware of which qubit is occupied by the past contextual gate. Fig. 3 shows an example. Gates can only be applied to the physical qubits in a free state. We call the gates whose associate physical qubits are all free as *lock free* gates.
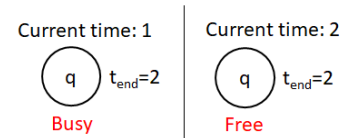

Fig. 3: Qubit lock t_{end} of qubit q is 2 means q is busy until time 2.

Qubit lock also makes CODAR aware of the gate duration difference. Different gate kinds have different duration and CODAR updates the operated qubit's lock t_{end} with different values. As a result, qubits occupied by gates with shorter duration will be set smaller t_{end} and become free earlier. Thus CODAR can use those earlier free qubits to route two-qubit gates and improve the parallelism of the program. As the example shown in Fig. 2 (d), suppose the program starts at time 0 and $\tau_T = 1$, $\tau_{CNOT} = 2$. Then t_{end} of Q_1 is set to 1 while t_{end} of Q_0 and Q_2 are set to 2. Q_1 becomes free at time 1 while Q_2 is still busy. CODAR can use Q_1 to route for the third gate and need not wait for the freedom of Q_2.

B. Commutativity Detection

Qubit lock brings CODAR awareness of the past contextual gate. On the other hand, considering gate commutation relation can expose more future contextual gate for CODAR to decide routing path.
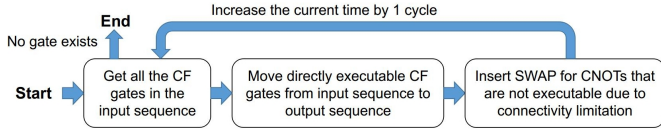
Fig. 4: Overview of the remapping algorithm.

Fig. 5: Example of the remapping process in one cycle.

Definition 1 (Commutative Forward Gate, CF gate). *Given a gate sequence $I=[g_1, g_2, ..., g_k, ...]$, $\forall g_k \in I$, g_k is a commutative forward gate iff $\forall j, 0 < j < k$, g_j and g_k are commutative.*

The commutation relation between two-qubit gates g_A, g_B that share qubits with each other can be resolved by checking the relevant unitary operators $\hat{A}\hat{B} = \hat{B}\hat{A}$. Gates applied to disjoint qubits are obviously commutative with each other.

All the CF gates in sequence I are denoted as I_{CF}. CF gates can be moved to the the head of I, which means they can be *executed instantly* from logical perspective. Compared to the methods that ignore the commutativity between quantum gates, choosing CF gates as logically-executable gates can expose more contextual gates for the heuristic search to determine better remapping solutions.

For example, suppose a sequence I contains two gates: CX q1,q3 and CX q2,q3 in order. The second gate shares q3 with the first and might not be regarded as logically executable due to qubit dependence. However, because the second commutes with the first one, both of the gates are CF gates in I and instantly executable in fact. Commutativity detection will expose both CXs for the heuristic search which improve the contextual look-ahead ability of CODAR.

C. Algorithms for CODAR Remapping

Now we discuss how CODAR transforms the quantum circuit to fit the hardware limitation. Given the coupling graph $\mathbb{M} =(Q, \mathsf{E}_H)$, initial mapping π and gate duration map τ, our algorithm takes an original gate sequence I as input, and generates an executable gate sequence $\mathcal{E}$. The overview of the algorithm is shown in Fig.4. The algorithm starts with the current time and each qubit lock initialized as 0. There are three steps in each iteration.

a) Step 1: At the start of each cycle, the algorithm first gets all CF gates in the input sequence I denoted as I_{CF}. The algorithm will terminate if there is no gate in I.

b) Step 2: In this step, the algorithm will select all directly executable gates in I_{CF}. A gate g is directly executable only when it satisfies two conditions below.

- g is a *lock free* gate.
- If g is a two-qubit gate like CNOT, its two target qubits are connected in the coupling graph.

Then the algorithm will apply those executable gates by moving them from the input sequence I to the output sequence $\mathcal{E}$ and update the qubit lock for each gate in the way described in Section IV-A.

c) Step 3: For the remaining CNOTs in I_{CF}, due to the connectivity limitation, the algorithm need decide which SWAPs should be inserted into the output sequence. The algorithm first searches all *lock free* edges associated with the qubits of each two-qubit gate g in I_{CF} to avoid huge overhead cost by global searching. For example, suppose g as "CX q_0, q_1", $Q_k = \pi(q_1)$ is the corresponding physical qubit of q_1 and we locate all of Q_k's adjacent qubits as $Q_{k1},Q_{k2},...,Q_{kt}$. Since the number of physical qubits may be greater than that of logical qubits, not every physical qubit has a corresponding logical qubit, thus the SWAP operation can only be applied to physical qubits. If the SWAP between Q_k and Q_{ki} ($1 \le i \le t$) is *lock free*, then SWAP Q_k,Q_{ki} will be regarded as a candidate. We repeat this process for all qubits associated with gate g to get the candidate SWAP set denoted as C_{swap}.

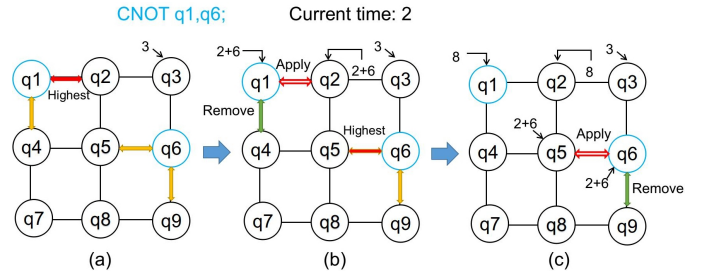Next, the algorithm repeatedly select the best SWAP in C_{swap} and insert it into $\mathcal{E}$ until no positive-priority SWAP remains in C_{swap}. The priority of a SWAP denotes the benefit it can bring to the circuit and we discuss how to calculate the priority for each SWAP in next subsection. In each selection iteration, the algorithm first calculates the priority for each g_{swap} in C_{swap}. Then the algorithm inserts the gate with the highest priority in C_{swap} into $\mathcal{E}$ and updates the qubit locks to remove the no longer *lock free* SWAPs from C_{swap}.

An example shown in Fig.5 illustrates the remapping process. Suppose a CNOT between qubits q1 and q6 need be applied at cycle 2 in a 3 × 3 grid model. For an easy explanation, we suggest in this cycle all qubit locks are 0 except the lock of qubit q3 is 3, which means that q3 is busy. As shown in Fig.5(a), the algorithm inspects each free edge associated with q1, q6 and calculates their priority. Because the lock of q3 is larger than the current time, the edge between q3 and q6 is not free. Finally, all the candidate SWAPs are colorized and suppose the red one has the highest priority. Then as shown in Fig.5(b), the algorithm applies the red one and updates the lock of qubit q1 and q2 (suppose the duration of SWAP is 6 cycle). This update causes the edge between q1 and q4 is no longer free, and it is removed from C_{swap}. The algorithm repeats the process and applies the SWAP between q5 and q6. In the end, no gate exists in C_{swap}, which leads to the termination of this cycle.

D. Design of Heuristic Cost Funtion

The heuristic cost function for SWAP g_{swap}

$$Heuristic(g_{swap}, \mathbb{M}, \pi) = \langle H_{basic}, H_{fine} \rangle$$

is to measure the benefits that gate g can bring to solve the mapping problem. When comparing the priority between two SWAPs, H_{basic} is compared first and H_{fine} is compared only when two gates have the same H_{basic}.

a) Basic Priority: Suppose a two-qubit gate g applied to logical qubits q_1 and q_2, $\mathbb{D} (\pi(q_1), \pi(q_2))$ denotes the distance of two qubits in the coupling graph $\mathbb{M}$. When the distance becomes 1, the gate fits the hardware limitation of the device.

$L(\pi,g)=\mathbb{D} (\pi(g.q_1), \pi(g.q_2))$ calculates the distance of $g \in I_{CF}$ based on the mapping π. To evaluate a candidate SWAP, we first temporarily use that SWAP to update π and get π_{new}. Then we calculate how much π_{new} can reduce (or increase) the distance of all $g \in I_{CF}$ compared to the original π. Equation 1 shows the basic priority heuristic function H_{basic}.

$$H_{basic} = \sum_{g \in I_{CF}} L(\pi, g) - L(\pi_{new}, g) \tag{1}$$

If the basic heuristic function of a specific SWAP ≤ 0, this SWAP won't shorten the total distance and cannot bring any benefit to the circuit. If we find no SWAP has a positive basic heuristic, there is no best SWAP gate. But sometimes it happens that neither SWAP gate nor other executable gates could be launched while all qubits are free. Such situations are called "deadlock" by us, and at this time we should just choose a SWAP with the highest priority to launch, even if its H_{basic} may not be positive.
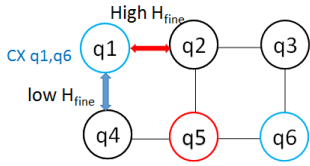
Fig. 6: The circuit is going to apply CX on q1 and q6 while q5 will be locked for a long time. The SWAP between {q1,q2} and between {q1,q4} have the same H_{basic}. But routing q1 through q4 will be blocked by q5 while routing through q2 can get better parallelism.
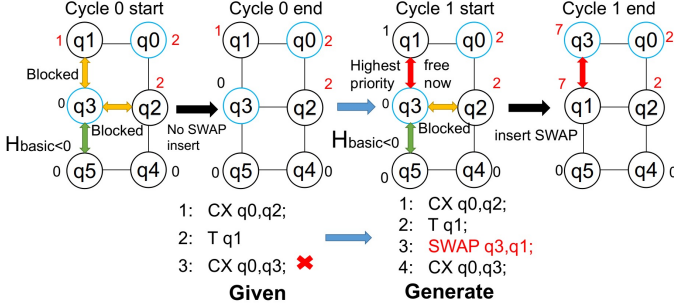

Fig. 7: Example of heuristic search for the high parallelism SWAP. The number near the qubits denotes the qubit lock t_{end}.

b) Fine Priority: In many cases, there are several candidate SWAPs with the same basic priority, so we design fine priority as shown in Equation 2 which applies to 2D lattice model.

$$H_{fine} = -|VD(\pi_{new}, g) - HD(\pi_{new}, g)| \tag{2}$$

Functions HD and VD stand for the horizontal and vertical distance on the lattice between the two qubits of g. The main idea of fine priority is: suppose a two-qubit gate g with specific distance $D = HD + VD$, there may be $C_D^{HD} = \frac{HD!VD!}{(HD+VD)!}$, possibly the shortest routing way for g, which increases as $|VD - HD|$ decreases. Choose a suitable SWAP gate to make $|VD - HD|$ smaller may let the remapping algorithm perform better in the future.

Retaining more possible routing way can improve the parallelism. Fig.6 shows a situation: H_{fine} indicates the algorithm to choose SWAP that can let the CX gate has closer vertical and horizontal distance which can avoid waiting for q_5 to be free.

E. Example

Now we use an example shown in Fig. 7 to explain our algorithm. Suppose there is a 6-qubit device and we are given a gate sequence I that contains a CX on {q0,q2}, a T on {q1} and a CX on {q0,q3}. The number near the qubit node represents the value of its t_{end}. All the three gates are CF gates. Due to the coupling limitation, CX on {q0,q3} is not directly executable and SWAP is needed. The algorithm simulates the execution timeline and starts at cycle 0.

At cycle 0, the first gate "CX q0,q2" and the second gate "T q1" are directly executable so both of them will be launched and qubits {q0,q1,q2}'s t_{end} locks are updated with the gate duration (T=1 cycle, CX=2 cycle). Each of {q0,q1,q2} has bigger t_{end} than current time and thus they are locked. Therefore the SWAP between {q1,q3} and {q2,q3} are blocked. SWAP between {q3,q5} with $H_{basic} < 0$ (which means the SWAP wont shorten the total distance of CF gates according to our heuristic cost function) moves q3 away from q0 and will not be inserted. As a result, no SWAP will be inserted in cycle 0 and the mapping π stays unchanged.

At cycle 1, qubit q1 becomes free while q2 stays busy. The SWAP between {q1,q3} becomes free while the SWAP between {q3,q2} is

still blocked. Therefore the algorithm knows that the SWAP between {q1,q3} can start earlier than SWAP between {q3,q2} and choose SWAP q3,q1 to solve the remapping problem. After launching "SWAP q1,q3", qubit locks of {q1,q3} are also updated by the sum of its start time (cycle 1) and the duration of SWAP (6 cycle) as 7.

V. EXPERIMENTAL EVALUATION

In this section, we evaluate CODAR with benchmarks based on the latest reported hardware models.

a) Comparison with Previous Algorithms: Several recent algorithms proposed by IBM [14], Siraichi *et al.* [26], Zulehner *et al.* [35] and Li *et al.* [18] try to find solutions of the qubit mapping problem with small circuit depth. Among them, Li's SABRE [18] beats the other three in the performance of benchmarks, thus it is used for comparison in this paper.

b) Hardware Configuration: We test our algorithm on several latest reported architectures, including IBM Q20 Tokyo[18], IBM Q16 Melbourne[1], 6×6 grid model proposed by Enfield [26]'s GitHub and Google Q54 Sycamore [3]. The gate duration difference configuration is based on experimental data of symmetric superconducting technology shown in Table I, where two-qubit gate duration is generally twice as much as that of the single-qubit gate.

c) Benchmarks: To evaluate our algorithm, we totally collect 71 benchmarks which are selected from the previous work, including: 1) programs from IBM Qiskit [9]'s Github and RevLib [31]; 2) several quantum algorithms compiled from ScaffCC [2] and Quipper [13]; 3) benchmarks used in the best-known algorithm SABRE [18]. The size of the benchmarks ranges from using 3 qubits up to using 36 qubits and about 30,000 gates. For the IBM Q16, Q20 and 6×6 architectures, 68 benchmarks out of the 71 benchmarks except 3 36-qubit programs are tested. While all 71 benchmarks are tested on Google Q54 Sycamore.
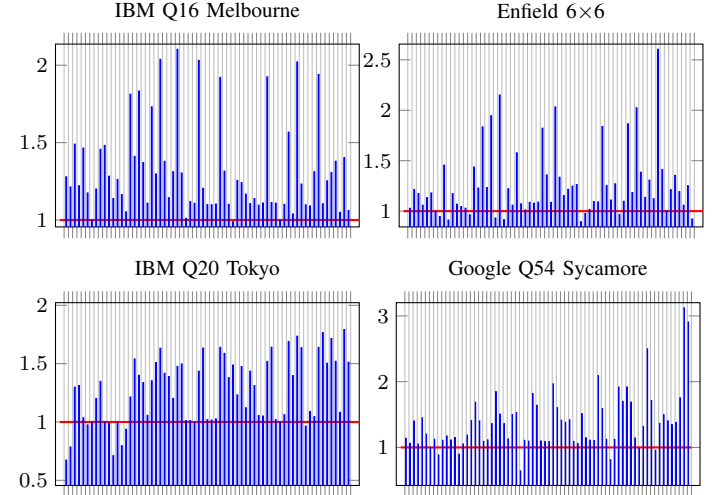

Fig. 8: Speedup ratio of all 71 benchmarks compared between CODAR and SABRE in four architectures. The benchmarks are listed from left to right in the ascending order of the number of qubits used.

A. Circuit Execution Speedup

We collect the weighted circuit depth of the circuits produced by CODAR and SABRE for the 71 benchmarks. Initial mapping has been proved to be significant for the qubit mapping problem, and for a fair comparison, we use the same method as SABRE to create the initial mapping for the benchmarks. We use the depth of circuits produced by SABRE compared with the one of CODAR to show the ability of our algorithm to speed up the quantum program. As shown in Fig.8,

the average speedup ratio of CODAR on four architecture models, IBM Q16 Melbourne, Enfield 6×6, IBM Q20 Tokyo and Google Q54 are respectively 1.212, 1.241, 1.214 and 1.258.

B. Fidelity Maintenance

Fidelity has been proved to be significant for the quantum computer in NISQ era. CODAR focuses on exploring the parallelism of the program to reduce the execution time and ignores the number of SWAPs inserted into the program. Compared to SABRE, CODAR may insert more SWAPs, which may bring more noise to the program. However, less execution time will improve the fidelity of the circuit on the contrary. To show CODAR's ability to maintain the fidelity, we use a distributed noisy quantum virtual machine made by Origin Quantum [24], which is based on Qubit Dephasing and Damping model [22] to simulate the fidelity of 7 famous quantum algorithms. The result (Fig.9) indicates that CODAR can speed up the circuits and maintain the fidelity of the circuits at the same time.
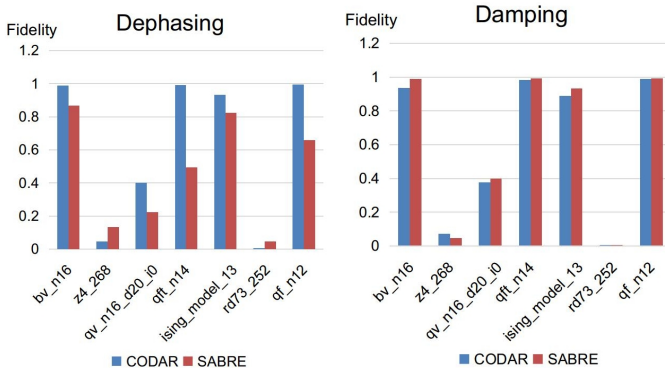

Fig. 9: Fidelity of the circuit produced by CODAR and SABRE for several quantum algorithms. When the noise mainly caused by qubit dephasing, CODAR performs better than SABRE and the fidelity of several circuits produced by CODAR reach nearly 1. When the noise mainly caused by qubit damping, CODAR performs about the same with SABRE.

VI. CONCLUSION

In NISQ era, most quantum programs are not directly executable because two-qubit gates can be applied between arbitrary two logical qubits while it can only be implemented between two adjacent physical qubits due to hardware constraints. To solve this problem, In this paper we propose CODAR that can transform the original circuit and insert necessary SWAP operations making the circuit comply with the hardware constraints. With the design of qubit lock and commutativity detection, CODAR is aware of the program context and the gate duration difference, which help CODAR remapper find the remapping with good parallelism and reduce QC's weighted depth. Experimental results show that CODAR remapper can speed up quantum programs by 1.212~1.258 in different quantum architectures compared with the best known algorithm on average and maintain the fidelity of the benchmarks when running on OriginQ quantum noisy simulator.

ACKNOWLEDGEMENT

REFERENCES

[1] IBM Q backend information. https://github.com/Qiskit/ibmq-device-information, visited in May 2019.
[2] Ali Javadi Abhari, Shruti Patil, Daniel Kudrow, Jeff Heckey, Alexey Lvov, Frederic T. Chong, and Margaret Martonosi. ScaffCC: A framework for compilation and analysis of quantum computing programs. In *11th CF*, pages 1:1–1:10, New York, NY, USA, 2014. ACM.
[3] Frank Arute, Kunal Arya, et al. Quantum supremacy using a programmable superconducting processor. *Nature*, 574:505–510, 2019.
[4] Abdullah Ash-Saki, Mahabubul Alam, and Swaroop Ghosh. QURE: Qubit re-allocation in noisy intermediate-scale quantum computers. In *56th DAC*, pages 141:1–6, 2019.
[5] Anirban Bhattacharjee, Chandan Bandyopadhyay, Robert Wille, Rolf Drechsler, and Hafizur Rahaman. A novel approach for nearest neighbor realization of 2D quantum circuits. In *ISVLSI*, pages 305–310. IEEE, 2018.
[6] Debjyoti Bhattacharjee and Anupam Chattopadhyay. Depth-optimal quantum circuit placement for arbitrary topologies. *arXiv preprint arXiv:1703.08540*, 2017.
[7] Kyle E. C. Booth, Minh Do, J. Christopher Beck, Eleanor Rieffel, Davide Venturelli, and Jeremy Frank. Comparing and integrating constraint programming and temporal planning for quantum circuit compilation. In *28th ICAPS*, pages 366–374, 2018.
[8] Frederic T. Chong, Diana Franklin, and Margaret Martonosi. Programming languages and compiler design for realistic quantum hardware. *Nature*, 549:180187, 2017.
[9] Andrew Cross. The IBM Q experience and QISKit open-source quantum computing software. *Bulletin of the American Physical Society*, 2018.
[10] Andrew W. Cross, Lev S. Bishop, John A. Smolin, and Jay M. Gambetta. Open quantum assembly language. *arXiv:1707.03429*, 2017.
[11] S. Debnath, N. M. Linke, C. Figgatt, K. A. Landsman, K. Wright, and C. Monroe. Demonstration of a small programmable quantum computer with atomic qubits. *Nature*, 536:63–66, 2016.
[12] A Fuhrmanek, R Bourgain, Yvan RP Sortais, and Antoine Browaeys. Free-space lossless state detection of a single trapped atom. *Physical Review Letters*, 106(13):133003, 2011.
[13] Alexander S. Green, Peter LeFanu Lumsdaine, Neil J. Ross, Peter Selinger, and Benoît Valiron. Quipper: a scalable quantum programming language. In *34th PLDI*, pages 333–342. ACM, 2013.
[14] IBM. QISKit. https://qiskit.org/, visited in Jan 2019.
[15] Abhoy Kole, Kamalika Datta, and Indranil Sengupta. A heuristic for linear nearest neighbor realization of quantum circuits by SWAP gate insertion using N-gate lookahead. *IEEE Journal on Emerging and Selected Topics in Circuits and Systems*, 6(1):62–72, 2016.
[16] Abhoy Kole, Kamalika Datta, and Indranil Sengupta. A new heuristic for N-dimensional nearest neighbor realization of a quantum circuit. *IEEE Transactions on Computer-Aided Design of Integrated Circuits and Systems*, 37(1):182–192, 2018.
[17] Harry Levine, Alexander Keesling, Giulia Semeghini, Ahmed Omran, Tout T Wang, Sepehr Ebadi, Hannes Bernien, Markus Greiner, Vladan Vuletić, Hannes Pichler, et al. Parallel implementation of high-fidelity multiqubit gates with neutral atoms. *Physical Review Letters*, 123(17):170503, 2019.
[18] Gushu Li, Yufei Ding, and Yuan Xie. Tackling the qubit mapping problem for NISQ-era quantum devices. In *24th ASPLOS*, pages 1001–1014. ACM, 2019.
[19] Norbert M. Linke, Dmitri Maslov, Martin Roetteler, Shantanu Debnath, Caroline Figgatt, Kevin A. Landsman, Kenneth Wright, and Christopher Monroe. Experimental comparison of two quantum computing architectures. *Proceedings of the National Academy of Sciences*, 114(13):3305–3310, 2017.
[20] KM Maller, MT Lichtman, T Xia, Y Sun, MJ Piotrowicz, AW Carr, L Isenhower, and M Saffman. Rydberg-blockade controlled-not gate and entanglement in a two-dimensional array of neutral-atom qubits. *Physical Review A*, 92(2):022336, 2015.
[21] Prakash Murali, Jonathan M Baker, Ali Javadi Abhari, Frederic T Chong, and Margaret Martonosi. Noise-adaptive compiler mappings for noisy intermediate-scale quantum computers. In *24th ASPLOS*, pages 1015–1029, Providence, RI, USA, 2019. ACM.
[22] Michael A. Nielsen and Isaac L. Chuang. *Quantum Computation and Quantum Information*. Cambridge University Press, UK, 10th Anniversary edition, 2010.
[23] Angelo Oddi and Riccardo Rasconi. Greedy randomized search for scalable compilation of quantum circuits. In *CPAIOR*, pages 446–461. Springer, 2018.
[24] Origin Quantum. QPanda Quantum software development kit. http://www.originqc.com.cn/en/QPanda/download.html, visited in Nov. 2019.
[25] Cheng Sheng, Xiaodong He, Peng Xu, Ruijun Guo, Kunpeng Wang, Zongyuan Xiong, Min Liu, Jin Wang, and Mingsheng Zhan. High-fidelity single-qubit gates on neutral atoms in a two-dimensional magic-intensity optical dipole trap array. *Physical Review Letters*, 121:240501, Dec 2018.
[26] Marcos Yukio Siraichi, Vinícius Fernandes dos Santos, Sylvain Collange, and Fernando Magno Quintao Pereira. Qubit allocation. In *CGO 2018*, pages 113–125, New York, NY, USA, 2018. ACM.
[27] Robert Stockill, M.J. Stanley, Lukas Huthmacher, E. Clarke, M. Hugues, A.J. Miller, C. Matthiesen, C. Le Gall, and Mete Atatüre. Phase-tuned entangled state generation between distant spin qubits. *Physical Review Letters*, 119(1):010503, 2017.
[28] Swamit S Tannu and Moinuddin K. Qureshi. Not all qubits are created equal: a case for variability-aware policies for NISQ-era quantum computers. In *24th ASPLOS*, pages 987–999. ACM, 2019.

[29] Davide Venturelli, Minh Do, Eleanor Rieffel, and Jeremy Frank. Compiling quantum circuits to realistic hardware architectures using temporal planners. *Quantum Science and Technology*, 3(2):025004, 2018.

[30] Davide Venturelli, Minh Do, Eleanor G Rieffel, and Jeremy Frank. Temporal planning for compilation of quantum approximate optimization circuits. In *26th IJCAI*, pages 4440–4446, 2017.

[31] R. Wille, D. Groe, L. Teuber, G. W. Dueck, and R. Drechsler. RevLib: An online resource for reversible functions and reversible circuits. In *38th ISMVL*, pages 220–225, May 2008.

[32] Robert Wille, Lukas Burgholzer, and Alwin Zulehner. Mapping quantum circuits to IBM QX architectures using the minimal number of SWAP and H operations. In *56th DAC*, page 142. ACM, 2019.

[33] Robert Wille, Oliver Keszocze, Marcel Walter, Patrick Rohrs, Anupam Chattopad-hyay, and Rolf Drechsler. Look-ahead schemes for nearest neighbor optimization of 1D and 2D quantum circuits. In *21st ASP-DAC*, pages 292–297. IEEE, 2016.

[34] K. Wright, K. M. Beck, S. Debnath, J. M. Amini, Y. Nam, N. Grzesiak, J. S. Chen, N. C. Pisenti, et al. Benchmarking an 11-qubit quantum computer. *arXiv e-prints*, page arXiv:1903.08181, Mar 2019.

[35] A. Zulehner, A. Paler, and R. Wille. An efficient methodology for mapping quantum circuits to the IBM QX architectures. *IEEE Transactions on Computer-Aided Design of Integrated Circuits and Systems*, 38(7):1226–1236, July 2019.